

# NUMERICAL REBUILDING OF DYNAMIC INSTABILITIES AND FORCES IN MULTIPHASE PIPE BEND FLOW

ANDREAS MACK, HRISHIKESH JOSHI & STEFAN BELFROID  
TNO Heat Transfer and Fluid Dynamics, Delft, The Netherlands.

## ABSTRACT

The present paper focusses on the numerical rebuilding of different multiphase flow regimes in a medium scale pipe system (6 inch). Principal investigations are performed by CFD to initiate hydrodynamic instabilities and develop them into the correct flow pattern (slug, stratified, etc.) at a given downwind position without applying artificial models or boundary conditions.

The numerical predictions of the flow obtained by a volume of fluid CFD method (OpenFoam) are compared with available experimental data. Numerical investigations are performed with respect to grid resolution, initial conditions and turbulence modelling but also for obtaining a representative, comparable set of numerical and experimental data.

For different flow regimes from slug flow to stratified flow good agreement with the experimental data was achieved with respect to the predicted flow regime and topology but also the forces predicted on the bend. Especially the large variation of the root mean squared values but also peak-to-peak values of the forces are predicted well by the numerical solutions for the different flow regimes.

*Keywords:* CFD, flow regimes, forces on bends, Multiphase flow, OpenFoam, VOF.

## 1 INTRODUCTION

In industrial multiphase applications like piping systems, not only an accurate prediction of the flow regime but also the forces acting on bends is essential designing installations while avoiding vibrational excitation of the system and possible damage or failure during operation. To assess structural integrity, often predefined, estimated liquid hold-up signals and/or forces based on the expected flow regime are taken as input for the structural analysis. At TNO, a large experimental database including a wide range of multiphase flow regimes in a 6" pipe with bends is available. This includes detailed hold-up and force data, which serves as database for force predictions in piping systems but also as validation database for CFD calculations [1, 2]. Recently, some of the cases have been rebuilt successfully by commercial CFD codes [3, 4]. The present work focusses on the prediction of the different flow topologies resolving Kelvin Helmholtz instabilities on the gas liquid interface [5] and an accurate estimation of the forces in the bends by an open source CFD code (OpenFoam). Special emphasis will be put on the level of detail which is required with respect to mesh resolution, geometrical features, inflow and initial conditions but also turbulence modelling to successfully model these kind of multiphase flows.

## 2 EXPERIMENTAL SETUP AND DATA

The experiments have been performed in the multiphase flow loop at TNO [1]. An overview of the experimental setup is given in Fig. 1. The flow loop facility has a gas system consisting of four compressors delivering gas through three flow measurement streets at a maximum gauge pressure of 7.5 bar. The gas is injected via a 4" Y-piece into the test loop. The test loop itself is an extension to the water loop. This fixed loop is build out of a main separator and three metering streets between two buffer vessels. The test loop consists of approximately 12m (~78 D) of horizontal pipe including a tomography section and an optical window for video. Downstream of the measurement bend the piping loops around the upstream

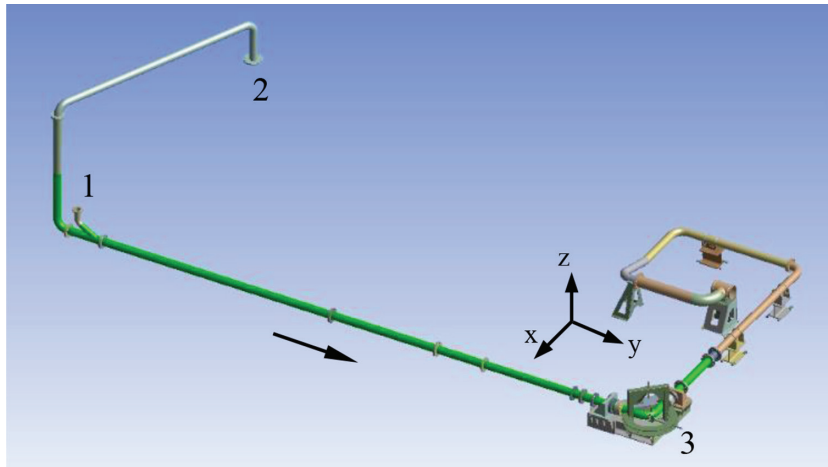


Figure 1: Experimental setup including gas injection (1), liquid flow line (2) and measurement bend (3); simulation domain marked in green; flow direction is indicated.

buffer vessel. The main piping is 6" (ID = 150 mm) in diameter, but the test loop increases in diameter (8") before the vertical section returning to the main separator. The measurement bend has a bend radius of 1.5D.

Up- and down-stream of the measurement bend various sensors are installed including pressure, temperature, acceleration and force measurement. The different sensors can be subdivided in three main groups: one group to measure the multiphase flow behaviour, a second group to measure process conditions (pressure and temperature) and the third group to measure the force on the measurement bend. The multiphase flow behaviour is measured with two cameras and two electrical resistance tomography (ERT) pipe sensors (2-plane instruments). One sensor is located upstream and one downstream of the bend. The force on the bend is measured directly with special designed force rings, which are connected to the flanges of a fixed support. The force is also measured indirect via strain gauge bridges, dynamic strain gauges, 11 dynamic pressure measurements in the bend and an accelerometer on the bend (at the hoisting eye). The force rings have an uncertainty of  $\pm 10$  N, whereas the piezo strain gauges have a typical uncertainty of  $\pm 2$  N. For the force data only the dynamic part has been taken into account. The force rings are also influenced by small temperature effects. Therefore, the data were first detrended (linear trend). The resulting data is used for determining the RMS (root mean squared values) and PSD (power spectral densities). The tests considered here are given in Table 1 including the superficial velocities of the gas ( $u_{sg}$ ) and liquid ( $u_{sl}$ ) phase and the corresponding flow regime.

Table 1: Flow conditions experiments [2].

Test number	$u_{sg}$ [m/s]	$u_{sl}$ [m/s]	Pressure at bend [bar]	Flow regime (observation)
432	2.0	2.01	1.26	Slug
409	1.1	1.97	1.26	Slug
419	7.6	2.04	1.49	Annular/stratified
424	20.0	1.57	1.82	Annular/stratified

### 3 NUMERICAL METHOD

OpenFoam is an open source C++ library containing a wide range of solvers and utilities for CFD applications. In the recent years, it has become a widely used alternative to other codes such as Fluent or Star-CCM, apart from classical one phase flow it has also been demonstrated to be reliable for multiphase applications. The class of interFoam solvers can handle compressible or incompressible two-phase flow problems by applying an interface capturing technique based on the volume of fluid method (VOF). Validation has been performed for a wide range of multiphase problems, recently also for different flow regimes in pipe flow including validation for liquid hold-up and pressure drop [5–8]. For the present study the compressibleInterfom solver of OpenFoam 2.3.0 was used which can handle compressible, non-isothermal immiscible liquid or gaseous phases. The solver is second order accurate in time and space. As turbulence closure, standard RANS (Reynolds averaged Navier–Stokes) and LES (large eddy simulation) turbulence models are available.

For the present simulations, the  $k-\omega$  SST model was applied for the RANS simulations and the Smagorinsky–Lilli subgrid scale model for LES computations. Within the VOF method, a compressive interfacial treatment of the liquid fraction advection was applied, the solution of momentum and pressure is done applying the Pressure Implicit with Splitting of Operators (PISO) pressure scheme including a velocity field predictor; as time stepping schemes Euler or backward are available with constant or variable time steps defined by maximum CFL numbers of the flow or interface.

### 4 NUMERICAL MODELLING SLUG FLOW (CASE 432)

For principal investigations of Kelvin Helmholtz instabilities on the gas/liquid interface developing into a certain flow regime conditions in the slug flow regime were chosen. For the conditions of case 432 of the test series ( $u_{sl}$  2.01 m/s and  $u_{sg}$  2.0 m/s) the bend was removed and the pipe length increased to get more insight into the development of the flow. In a second step, the bend was included to assess the forces.

#### 4.1 Principal Investigations

The domain consists of a 20 m long pipe (6" = 0.1524 m diameter) with a 30° tilted, lateral gas injection port (diameter 0.1 m) in the center of origin. Since the required pipe length to achieve a fully developed multiphase flow pattern is unknown, not a generic stratified inflow was chosen but the gas injection was modelled. Due to the smaller diameter of the gas injection pipe compared with the main pipe, the velocity difference at the interface is maximized such that instabilities can be triggered earlier.

The bend, which is not simulated here, would be at a downstream position of 12 m. The domain length is increased in order to get a principal idea of the development of the flow from the gas injection downstream. Only half of the domain was simulated applying symmetry boundary conditions in lateral direction.

The mesh resolution in the cross section was chosen comparable to other investigations (5 wall normal cells to resolve the boundary layer, first cell 1 mm spacing, 5 mm cell size in the pipe core, 40 cells in circumferential direction), the resolution in longitudinal direction (away from the gas injection) was chosen after numerical testing to 0.02m.

As boundary conditions a fixed mass flow rate was applied to the gas inlet and a constant velocity to the liquid inlet. The static pressure at the outlet was fixed to 1.2 bar. As initial

condition, the whole domain was filled with liquid and the computations were performed applying the  $k-\omega$  SST turbulence model (RANS).

The time accurate computations were run until a quasi-periodic solution was achieved and sufficient data were collected for post processing. This is typically 10 s until the sampling is started, which should last at least 20 s for the present slug cases to achieve a reasonable representation of the low frequency features. Comparing the results of the liquid hold-up data obtained from the numerical solution with the experimental results shows that the CFD solution can reproduce the slugging behaviour for the chosen flow condition. Slugs are formed with a non-regular distribution in time comparable to the experimental data. The numerical solution shows less periods of a completely filled pipe and the minimum values of 0.3 are achieved less often (Fig. 2).

When comparing the numerical data at 12 m and 20 m, no large differences can be seen. The hold-up is slightly smoothed and the minimum and average values increase slightly possibly also due to the change in pressure.

All observations with the time dependent signal can be confirmed by the time averaged hold-up data (Table 2). The time averaged hold-up from the numerical simulation agrees well with the experimental data post-processed applying the linear interpolation method (explained later in chapter 4.3) and is increasing at further downstream locations. The standard deviation has also a good agreement and is slightly decreasing further downstream.

The power spectral density of the liquid hold-up signals is given in Fig. 3. The frequency distribution of the slugs shows a nice agreement with the experimental data. Comparable to the experimental data, the maximum of the distribution is at approximately 0.7 Hz and the values agree reasonably. For the very low frequency range (<0.5 Hz) the overall sampling time available is too short to get a representative distribution. Between  $x = 12$  m and 20 m the distributions do not change significantly. According to these results, it can be summarized

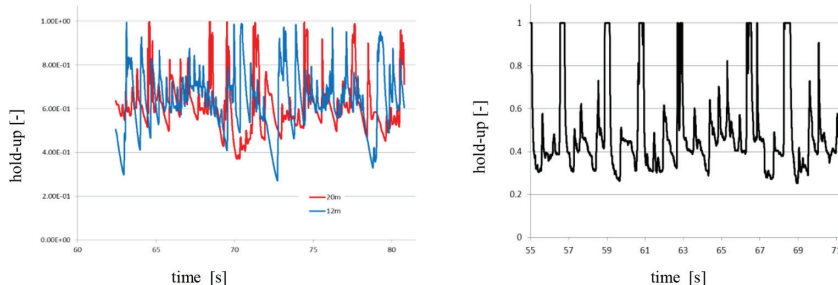


Figure 2: Hold-up signal upstream of bend, numerical data (left) and experimental data (right).

Table 2: Experimental and numerical hold-up data for slug case 432

Case	Hold-up [-]	Standard deviation [-]
Exp. 432	0.48	0.19
Exp. 432 (linear interpol.)	0.59	0.15
CFD $x = 12$ m	0.59	0.16
CFD $x = 20$ m	0.63	0.11

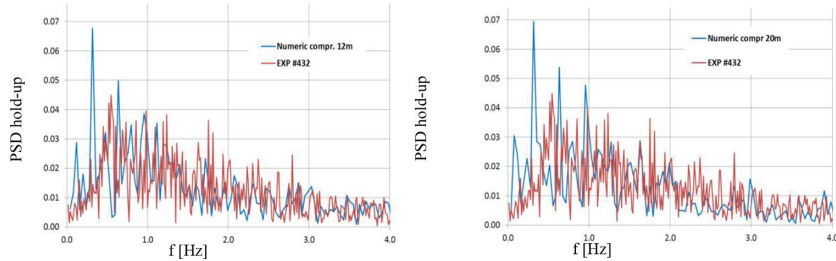


Figure 3: Power spectral density of hold-up signal over frequency of experimental data (upstream of bend) compared with the numerical solution at  $x = 12\text{ m}$  (left) and  $x = 20\text{ m}$  (right).

that the correct flow topology can be modelled numerically by CFD with good agreement by developing irregular slugs from Kelvin Helmholtz instabilities. Since slugs can be damped at further downstream positions, the correct upstream length of the pipe has to be ensured but also geometrical features must be taken into account when predicting forces on bends. Simple boundary conditions with stratified inflow will result in very long pipe lengths for fully developed slug flow patterns since the velocity difference of the gas and liquid phase is low.

#### 4.2 Numerical modelling including pipe bend

Since the numerical prediction of the forces generated by multiphase flow in a pipe bend is the final interest of the present study, the geometry was updated with the bend. It consists of the geometry explained before with the gas injection, the downstream horizontal bend and a final 2m downstream section. At the liquid inflow a 1m section with the vertical bend was also included in the simulation (compare also Fig. 1).

For this configuration, various numerical sensitivities were investigated. A grid refinement study was performed but due to the computational effort no full grid refinement including refinement in all directions could be chosen. The grids were refined in the cross sections (including increased wall normal resolution) and mainly in axial direction (with minor refinement in the cross section). The standard mesh consisted of a comparable resolution of the semi domain discussed before; the mesh sizes and metrics used are given in Table 3.

Initial and boundary conditions were identical to the previous case. According to these results of the numerical simulations on different meshes, the predicted values for the average hold-up and standard deviation (Tables 4 and 5) are not very sensitive to the different grid resolution. All solutions over predict the average hold-up signal and underestimate the standard variation consistently.

Table 3: Mesh metrics for mesh refinement study.

Mesh	Cells	Nodes	Prism layers (wall normal direction)	1 <sup>st</sup> wall normal spacing	Cells in cross section	Axial resolution
Reference	920.000	852.000	5	1 mm	900	0.02 m
Refined BL	$1.26 \cdot 10^6$	$1.45 \cdot 10^6$	10	0.25 mm	1200	0.02 m
Refined axially	$2.15 \cdot 10^6$	$1.8 \cdot 10^6$	5	1 mm	1050	0.01 m

Table 4: Grid refinement study, numerical hold-up data upstream of bend for slug case 432 (\*applying 75% threshold on signal in postprocessing).

Case	Hold-up upstream [-]	Standard deviation [-]
Reference RANS	0.683	0.146
Refined BL (RANS)	0.688	0.10
Refined axial (RANS)	0.665	0.126
Reference LES	0.663	0.122
Reference LES pp 75%*	0.629	0.118
Filling sim. (RANS)	0.577	0.202
EXP	0.48	0.19
EXP (linear interp.)	0.59	0.15

Table 5: Grid refinement study, numerical hold-up data downstream of bend for slug case 432 (\*applying 75% threshold on signal in postprocessing).

Case	Hold-up downstream [-]	Standard deviation [-]
Reference RANS	0.591	0.234
Refined BL (RANS)	0.536	0.198
Refined axial (RANS)	0.549	0.199
Reference LES	0.551	0.157
Reference LES pp 75%*	0.453	0.152
Filling sim. (RANS)	0.511	0.235
EXP	0.47	0.27
EXP (linear interp.)	0.51	0.21

In accordance with the experimental data, the liquid hold-up is decreasing and the standard deviation is increasing over the bend (Tables 4 and 5). At the downstream position, the slugs are more regularly compared with the upstream position. Upstream the bend, the slugs are built up, at times it takes 2 or 3 smaller slugs to build up a bigger one. The slug leading edge is quite sharp, whereas the tail is more shallow. Downstream the bend, the slugs are further developed with a more square wave signal. This behaviour is also present with the experimental data (compare Fig. 4).

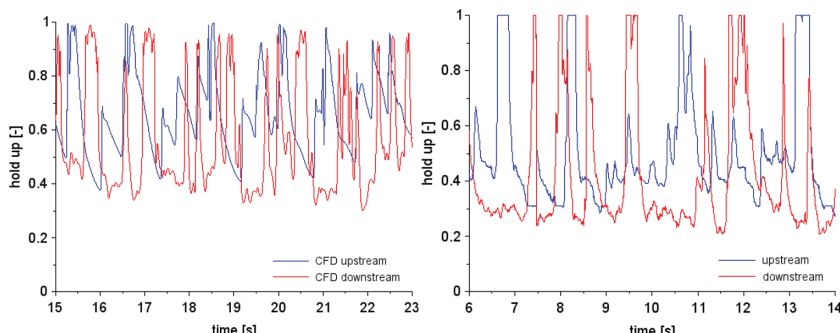


Figure 4: Hold-up data case 432 of numerical simulation (left, 'Reference RANS') and experimental data (right).

The agreement between the experimental and numerical data of the power spectral densities of the hold-up signals of with respect to frequency at the upstream position is good. The global maximum at approximately 0.7 Hz is reproduced well by the CFD solution. The experimental data shows some higher peaks at the position downstream the bend (Fig. 5) but the overall agreement can be considered good.

During the numerical calculation, the forces acting on the bend region including pressure and viscous components were sampled. The data was postprocessed and compared with the experimental data. In order to achieve comparable values to the experimental data, the forces were modified by subtracting its average values accordingly. By this, peak to peak values can be compared more easily. In addition, root mean squared values (RMS) of the x and y components were calculated and compared to the experimental data. In Table 6, the numerical and experimental values are compared. The ratio of the x and y components and the order of magnitude of the forces are predicted correctly by the numerical calculation, whereas the values of the RMS forces are underpredicted by approximately 30% by the numerical calculations. Also for the refined grids only a small variation in the predicted forces can be stated. According to these results, the meshes can be considered to have sufficient resolution to predict the present flow field reasonably.

The time dependant force data (RANS solution on reference grid) is compared in Fig. 6 with the experimental data. The forces for both x and y direction are approximately within +300 N and -200 N, the negative peaks of the numerical solution are slightly higher. The numerical solution predicts approximately the same force range; also the signal shape is in good agreement with the experimental data and the power spectral densities of the forces (Fig. 7) agree well in the relevant frequency range up to 50 Hz.

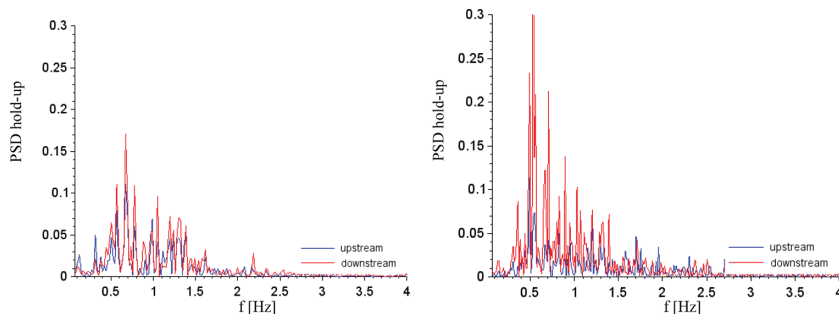


Figure 5: Power spectral density of hold-up (case 432), numerical data (left, ‘Reference RANS’) and experimental data (right).

Table 6: Grid refinement study, numerical force data for slug case 432.

Case	RMS $F_x F_y$ [N]	Ratio RMS $F_x/F_x$ [-]
Reference RANS	57 63	0.90
Refined BL (RANS)	59 63	0.94
Refined axial (RANS)	60 64	0.94
Reference LES	79 92	0.86
Filling sim. (RANS)	102 113	0.90
EXP	79 96	0.83

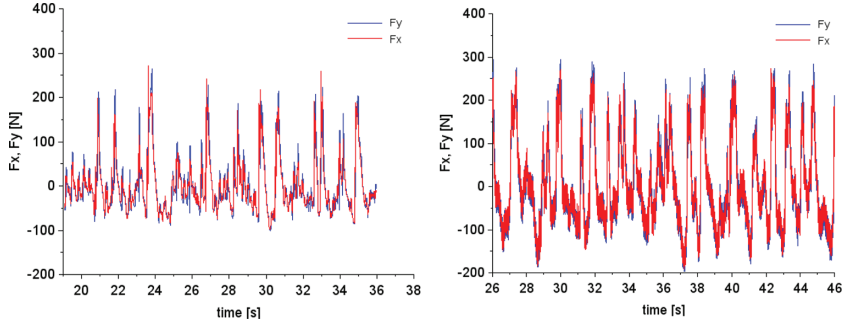


Figure 6: Force data case 432 from simulation (left, ‘Reference RANS’) and experiment (right).

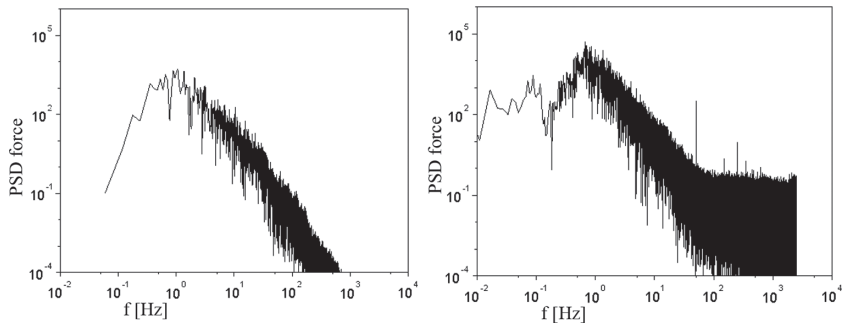


Figure 7: Power spectral density of forces ( $F_y$ ) of numerical solution (left ‘Reference RANS’) and experimental solution (right).

#### 4.3 Sensitivities

Although it was shown that the simulation captures the main flow features, a difference especially in the time averaged hold-up remains. As shown earlier the numerical signals (hold-up upstream of bend) are approximately 20% higher than the measured ones and the grid resolution cannot be the reason. Therefore, additional investigations were performed with respect to the numerical model, the signal processing but also the initial flow solution.

The postprocessing of the experimental data of the hold-up signal, obtained by tomography, is either done by linear interpolation or applying a 75% threshold value to the tomography integration cell [2]. In the latter case, it means that only the regions above that limit are considered. The resolution is approximately 20 pixels at the pipe diameter; therefore, the interfaces at regions including small liquid features are less resolved. Due to this, the liquid fraction will be underestimated by the experimental data. This is also observed for other experimental results with lower liquid hold-up where the liquid fraction behind the bend was dropping significantly or completely vanishing (see following chapters). Since the resolution of the computational mesh (away from the walls) and the thermography resolution are comparable, the liquid fractions during the computation were written out applying also a 75% threshold. Comparing the two numerical data with and without the threshold showed only minor differences of approximately 1 to 2% in smooth regions and not more than 10% in regions including smaller flow features. The average hold-up values differ less than 2%.

Latest postprocessing of the experimental data applying the linear interpolation method showed higher values for the hold-up and lower standard deviations (the experimental data is included in Table 4). Comparing the numerical data with these values shows a much better agreement upstream and downstream the bend. Therefore, the postprocessing of the experimental signal is the reason for the lower hold-up fraction of the experiment compared with the CFD model for the present slug case 432. Further on in this paper the experimental data of the hold-up signal are still based on the threshold method if not mentioned elsewhere.

For multiphase flow, also large eddy simulation (LES) is regularly used in literature reporting good results [3, 4]. Therefore, a LES model with the Smagorinsky Lilli subgrid scale model was applied for the present slug flow case 432. At the inflow, a turbulent inlet boundary condition (based on adding random fluctuations to mean field) was applied with 10% of RMS fluctuation scale and 10% fraction of new random component added to the one of the previous time step.

The time dependent liquid hold-up data of the LES solution does not differ significantly from the RANS data shown earlier and the average and standard deviation of the hold-up are slightly lower than the RANS data presented earlier (compare data in Table 4 and Table 5). Since the LES model resolves smaller vortices, full closing of the pipe due to slugs occurs less regularly at up- and down-stream positions. Due to the temporary accumulation of liquid in the bend higher peak-to-peak forces are observed (Fig. 8). The RMS value of the forces are predicted as  $F_x = 79$  N and  $F_y = 92$  N, which is an excellent agreement with the experimental value of 79 N and 96 N (Table 6).

With the LES simulations it was observed that the flow topology in the bend upstream of the gas injection showed minor differences with the RANS solutions; a slightly larger separation (and region with larger scale longitudinal vortices) was observed with the LES solution compared with the RANS resulting in a larger flow velocity and more horizontally aligned flow in the lower part of the pipe upstream of the gas injection. Therefore, the differences of the LES solution might partially be due to the different interaction of the liquid with the injected gas.

In addition, setting a homogenous inflow as boundary condition for liquid and gas is already a simplification. During start-up of the experiment, the gas is continuously injected in the pipe system while the liquid mass flow is slowly increased. Therefore, the liquid level is build up slowly and since the liquid is travelling through a vertical pipe section of several meters, a considerable volume of gas is present in that region. The water falls down and will

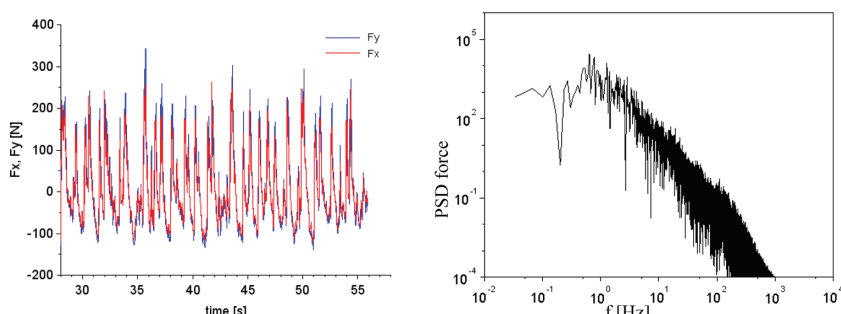


Figure 8: Force data (left) and power spectral density of force data (right) from simulation (LES, case 432).

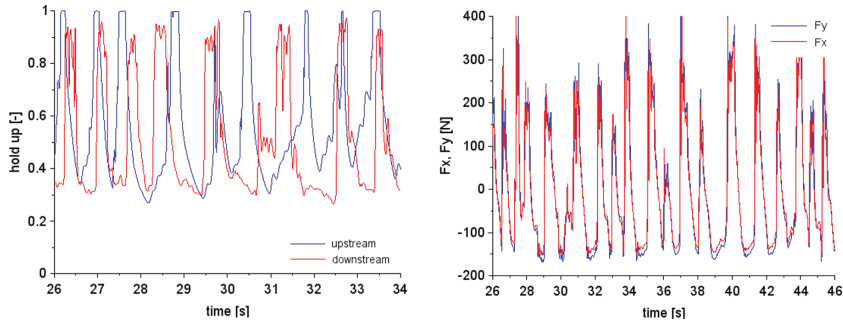


Figure 9: Liquid hold-up (left) and force data (right) of numerical RANS simulation including pipe filling process.

not fill the whole pipe immediately. Therefore, it is not clear whether the flow separation is present at all after the bend upstream of the gas injection or if a gas pocket is still present.

Computations were performed where the liquid was present in the vertical section of the pipe only; the remaining domain was initiated with gas. By this, the filling process of the horizontal pipe was simulated. The computations show that the liquid does not follow the bend creating counterrotating vortices but is falling vertically onto the lower surface of the horizontal pipe. Due to this, a gas pocket remains present between upstream the gas injection. In addition, the velocity increases due to additional potential energy. The horizontal pipe is slowly filled with water while a large velocity slip is present between liquid and fluid. After reaching a quasi-steady state liquid level of approximately 70% (liquid hold-up at the gas injection region), instabilities are observed further downstream the pipe but still upstream of the bend where also the slugs are initiated.

The results of the liquid hold-up are given in Fig. 9, the average and standard deviation values show an excellent agreement with the experimental data especially if compared with the experimental data based on the more accurate linear interpolation method (data already included in Tables 4 and 5, ‘filling sim. (RANS)').

The RMS forces are higher compared with the previous simulations and the experiments, the data are included in the previous Table 6.

The latest experimental force data showed forces of  $F_x = 99$  N and  $F_y = 105$  N for case 432 which is close to the numerical solution including the filling process. It might be that depending on the starting process of the experiment different flow patterns are obtained.

## 5 NUMERICAL MODELLING OF ANNULAR AND STRATIFIED FLOW CONDITIONS

Apart from slug flow, annular and stratified flow cases are of particular interest since the maximum forces on bends are typically observed at lower average hold-up but higher superficial gas velocities. For the available experimental data set, high RMS forces are measured for an annular flow case (case 419, liquid hold-up 0.25) and the maximum peak-to-peak forces for an annular flow case with a lower average hold-up (case 424, liquid hold-up 0.09). These two cases were selected to compare experimental and numerical data. An additional slug flow case was selected (case 409) to get more insight whether the numerical model can also predict slugging at a different flow condition. This case has a higher average hold-up (0.6) compared with the previous case (432) and shows strong, regular slugs/plugs, which pass the bend almost unchanged (compare Tables 7 and 8). The numerical solutions for all

Table 7: Numerical hold-up data upstream of bend for slug case 432 (\*applying 75% threshold on signal in postprocessing).

Case	EXP hold-up [-] stdev [-]	RANS hold-up [-] stdev [-]	LES hold-up [-] stdev [-]
409	0.60 0.27	*0.711 0.195	*0.717 0.142
409 (linear int.)	0.65 0.21	0.726 0.191	0.742 0.140
419	0.25 0.06		*0.244 0.054
419 (linear int.)	0.30 0.06	0.293 0.128	0.299 0.071
424	0.09 0.03	*0.066 0.060	*0.089 0.016
424 (linear int.)	0.15 0.03	0.141 0.109	0.151 0.021

cases were achieved from pipes initially fully filled with liquid. For all cases, the hold-up data are included in Tables 7 and 8, the force data in Table 9.

The numerical results of slug flow case 409 are correlating with the experimental results comparable to the previous case 432. The average liquid hold-up is over predicted by 12–13%, the standard deviation is under predicted by 8–10%. Comparing with the experimental data based on the linear interpolation method, the hold-up shows a difference of 8% and the standard variation of 2–3%. RANS and LES data do not show significant differences, also the postprocessing applying liquid fractions above 75% only shows minor differences since the slugs are quite large and compact. Downstream of the bend the slugs seem to be more decomposed applying an LES model since the liquid fraction is reduced downstream of the bend by 6% (applying the 75% threshold on the CFD hold-up signal). The slightly decreasing average hold-up absolute values and increasing variations over the bend are reproduced well. The liquid hold-up signals also agrees reasonably with respect to minimum and temporal behaviour, whereas no full closing of the pipe is observed with the numerical solution (Fig. 10).

Table 8: Numerical hold-up data downstream of bend for slug case 432 (\*applying 75% threshold on signal in postprocessing).

Case	EXP hold-up [-] stdev [-]	RANS hold-up [-] stdev [-]	LES hold-up [-] stdev [-]
409	0.58 0.30	*0.657 0.202	*0.640 0.166
409 (linear int.)	0.61 0.23	0.695 0.198	0.704 0.163
419	0.07 0.07		*0.200 0.062
419 (linear int.)	0.18 0.07	0.295 0.144	0.306 0.075
424	0.0 0.002	*0.069 0.057	*0.117 0.021
424 (linear int.)	0.098 0.022	0.149 0.092	0.204 0.117

Table 9: Force data (RMS) cases 409, 419 and 424.

Case	EXP F <sub>x</sub> F <sub>y</sub> [N]	RANS F <sub>x</sub> F <sub>y</sub> [N]	LES F <sub>x</sub> F <sub>y</sub> [N]
409	59 73	52 55	51 56
419	183 233	196 220	102 134
424	134 174	196 234	103 126

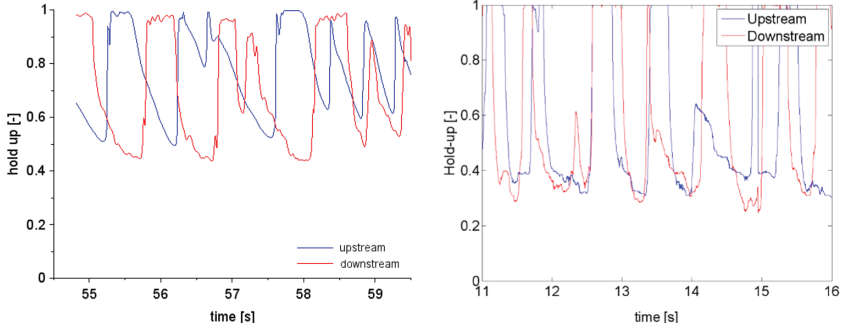


Figure 10: Liquid hold-up of RANS simulation (left) and experimental data (right) of flow case 409.

With respect to the forces, both RANS and LES under predict the RMS values (Table 9). Comparing the force signals of the RANS solution (Fig. 11), the peak maximum values are predicted with good agreement whereas the minimum peak values are slightly too high with the numerical solution. The agreement with respect to time can be considered as good.

The numerical results for the cases 419 and 424 indicate that the flow topology is rather stratified than annular as expected from the classical flow regime map. Taking a gravity corrected flow regime map [9] into account, the flow can be classified as ‘intermittent slug/plug’. Due to the relatively large pipe diameter the gravitational terms become dominant and the liquid tends to be accumulated at the bottom of the pipe. With both cases, instabilities occur at the liquid-gas interface, the instantaneous liquid fractions of the numerical solutions (RANS) are between 0.1 and 0.8 (case 419, Fig. 12) and 0.05 and 0.45 (case 424, Fig. 14). The experimental values of the average liquid hold-up decreases over the bend, whereas it stays approximately constant with the numerical solutions (Tables 7 and 8) and the processing of the experimental data, which is more accurate for larger absolute values. In principle, the liquid should not disappear over the bend. Due to this, a comparison of downstream data has to be done with care and only the experimental data based on the linear interpolation method shall be taken into account. For both cases, the liquid hold-up upstream of the bend is also over predicted by the numerical results. As the alternative postprocessing indicates (Table 7, case 424), the absolute values drop by 40% since the liquid entrains gas bubbles in

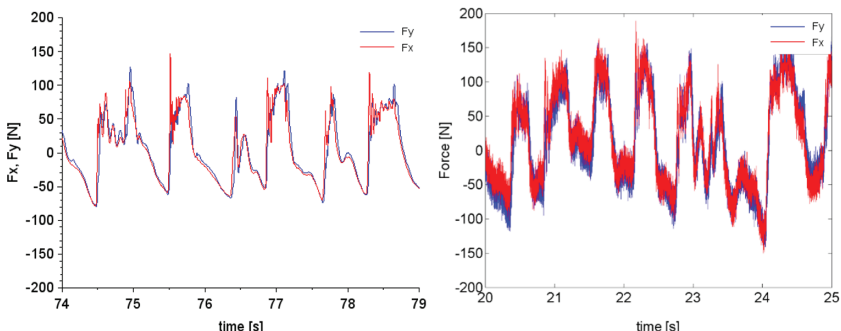


Figure 11: Force on bend data of RANS simulation (left) and experimental data (right) of flow case 409.

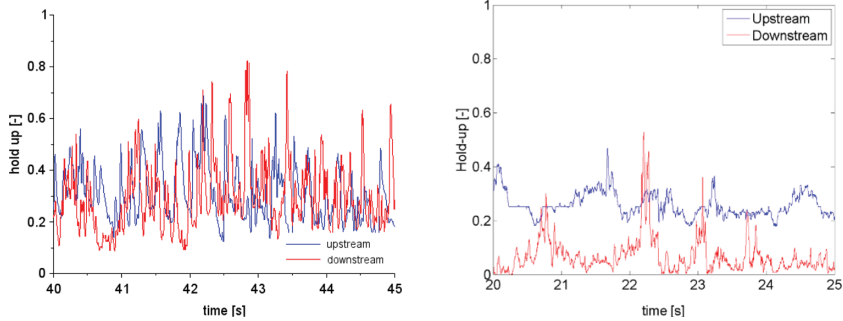


Figure 12: Liquid hold-up of RANS simulation (left) and experimental data (right) of flow case 419.

this domain. Comparing the experimental data bases on the linear method with the simulated hold-up data upstream the bend both RANS and LES solution show excellent agreement with the experimental data (Table 7, cases 419 and 424); the standard deviations are slightly over predicted by the RANS solutions and well or slightly under predicted by the LES solutions.

For case 419 (Fig. 12) it can be seen that both for experimental as numerical data the maximum instantaneous hold-up behind the bend is larger than upstream. Since the experimental data in this case is considered more reliable (larger liquid fractions) and the agreement of the liquid hold-up peaks is correlating with the force peaks (Fig. 13) it can be stated that small waves created on the liquid surface seem to be the reason for the force peaks. Investigating the numerical flow field, it can be shown that these small waves grow and eventually close the pipe at the bend where liquid is accumulated due to the redirection of the flow. This is the reason for the force peaks, which are an order of magnitude larger (Fig. 13) compared with the slug case 409. The peak-to-peak forces of case 424 are in the same order of magnitude as for case 419 and are predicted at slightly lower values numerically (Fig. 15). The coincidental peaks due to liquid accumulation are well resolved by CFD whereas the experimental force data looks more cyclic than the numerical one.

Despite the fact that the RANS model predicts slightly too strong slugs with higher hold-up variation at the position upstream of the bend (Table 7), the RMS force data are predicted well for case 419. For case 424, the force RMS values are still under predicted. With the LES

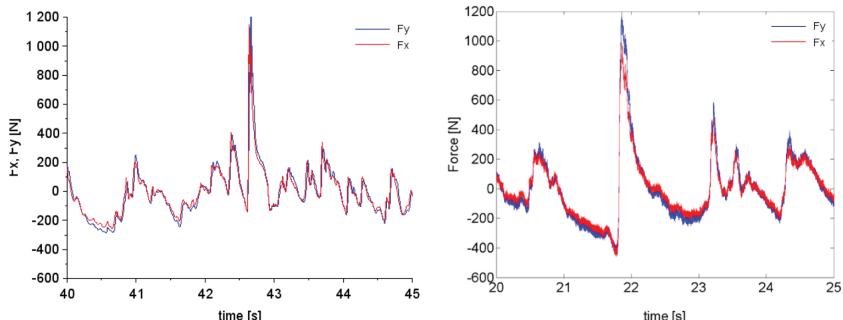


Figure 13: Force on bend data of RANS simulation (left) and experimental data (right) of flow case 419.

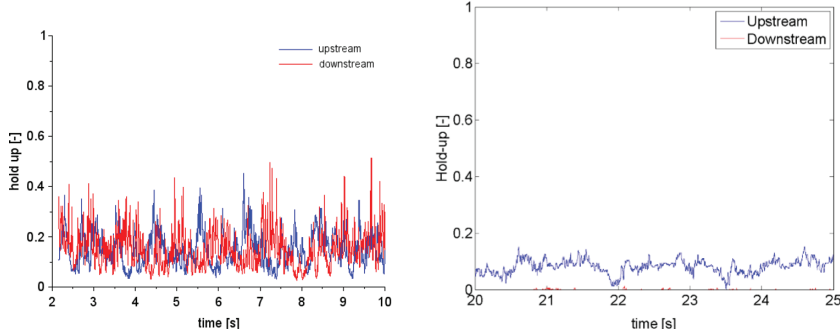


Figure 14: Liquid hold-up of RANS simulation (left) and experimental data (right) of flow case 424.

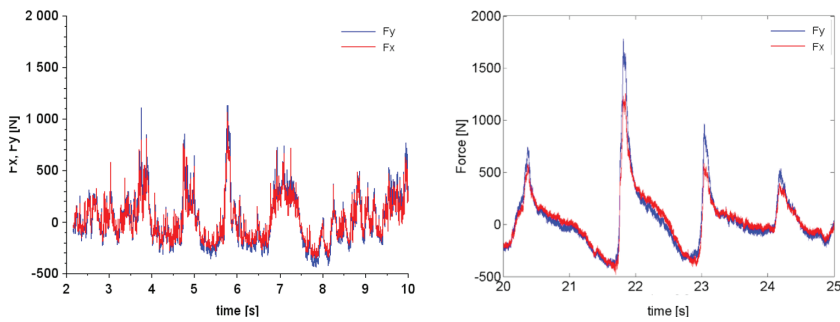


Figure 15: Force on bend data of RANS simulation (left) and experimental data (right) of flow case 424.

solutions too much gas seems to be entrained into the liquid which decomposes the larger wave structures, therefore the RMS force data is consistently under predicted. From these results, LES should not be recommended for this kind of flow (stratified with small liquid hold-up) in combination with the present mesh resolution and LES model. In principle, the mesh resolution should be significantly increased to resolve these small structures at the liquid/gas interface more accurately. With the RANS solutions larger structures are resolved and resulting in larger waves and larger flow features.

Although not all flow features might be resolved, the prediction of the forces with respect to the RMS values but also peak values can still be considered as good for the RANS solution. As explained earlier the initial solution (filling process of the pipe) might also play a role with the present cases, although less effect is expected since the flow is more developed before reaching the bend (stratified flow at lower average hold-up).

## 6 SUMMARY

For different multiphase flow conditions including slug and stratified flow CFD has been successfully applied to model the correct flow topologies in a 6" pipe including a bend. The numerical data obtained with OpenFoam has been validated with available experimental data with respect to liquid hold-up and the forces acting on the bend and shows good agreement for different flow cases.

For the slug flow cases, the LES turbulence closure showed slightly better agreement with the experimental data compared with the RANS solutions. For the stratified flow cases, the LES model could not reproduce the higher peak-to-peak force values due to a disintegration of larger slugs temporally present into smaller ones. Apart from the turbulence modelling, the initial conditions play a major role achieving the correct flow topology due to the presence of local gas pockets in the flow field.

#### ACKNOWLEDGEMENT

The experimental results were provided by the JIP project ‘Multiphase Flow Induced Vibration’ coordinated by Xodus. The experiments were mainly conducted in the TNO facilities. The authors would also like to acknowledge the sponsors BP, Shell, Statoil, Total, Lundin, AkerSolutions and FMC Technologies for the possibility to publish these results.

#### REFERENCES

- [1] Belfroid, S., Nennie, E., van Wijhe, A., Pereboom, H. & Lewis, M., *Multiphase forces on bend structures – overview large scale 6” experiments*. proceeding of 11th Conference on Flow-Induced Vibration and Noise, The Hague, The Netherlands, 4–6 July, 2016.
- [2] Belfroid, S.P.C. & Nennie, E., *JIP Forces on Bends due to multiphase flow (6”)*, TNO project report 24.03.2015, Delft, The Netherlands, 2015.
- [3] Emmerson, P., Lewis, M. & Barton, N., *Multiphase forces on bend structures- influence of upstream disturbance*. Proceeding of 11th Conference on Flow-Induced Vibration and Noise, The Hague, The Netherlands, 4–6 July, 2016.
- [4] Pontaza, J., Kreeft, J.J., Abuali, B., Smith, F.J. & Brown, G.W., *Flow-induced forces in piping due to multiphase flow: prediction by CFD*, The Hague, The Netherlands, 4–6 July 2016.
- [5] Vaze, M.J. & Banerjee, J., Experimental visualization of two-phase flow patterns and transition from stratified to slug flow. *Journal of Mechanical Engineering Science*, **225**, pp. 382–389, 2011.  
<https://doi.org/10.1243/09544062jmes2033>
- [6] Deshpande, S.S., Anumolu, L. & Trujillo, M.F., Evaluating the performance of the two-phase flow solver interFoam. *Computational Science & Discovery*, **5**(1), p. 014016, 2012.  
<https://doi.org/10.1088/1749-4699/5/1/014016>
- [7] Shuard, A.M., Mahmud, H.B. & King, A.J., Comparison of Two-Phase Pipe Flow in OpenFOAM with a Mechanistic Model. *IOP Conference Series: Materials Science and Engineering*, **121**, p. 012018, 2016.  
<https://doi.org/10.1088/1757-899x/121/1/012018>
- [8] Thaker J.P. & Banerjee J., *CFD simulation of two-phase flow phenomena in horizontal pipelines using openfoam*. Proceeding for the 40th National Conference on Fluid Mechanics & Fluid Power (Hamipur) FMFP2013 paper 34, 2013.
- [9] McCaslin, J. & Desjardins, O., Numerical investigation of gravitational effects in horizontal annular liquid–gas flow. *International Journal of Multiphase Flow*, **67**, pp. 88–105, 2014.  
<https://doi.org/10.1016/j.ijmultiphaseflow.2014.08.006>